Reflectionless propagation of Manakov solitons on a line: A model based on the concept of transparent boundary conditions

K. K. Sabirov,[1,2] J. R. Yusupov,[3] M. M. Aripov,[4] M. Ehrhardt,[5] and D. U. Matrasulov[3,6]

[1]*Tashkent University of Information Technologies, Algorithms and Mathematical Modeling, 108 Amir Temur Street, Tashkent 100200, Uzbekistan*

[2]*Tashkent State Technical University, Higher Mathematics, 2 Universitet Street, Tashkent 100095, Uzbekistan*

[3]*Yeoju Technical Institute in Tashkent, 156 Usman Nasyr Street, Tashkent 100121, Uzbekistan*

[4]*National University of Uzbekistan, Applied Mathematics and Computer Analysis, 2 Universitet Street, Tashkent 100095, Uzbekistan*

[5]*Bergische Universität Wuppertal, Applied Mathematics and Numerical Analysis, Gaußstrasse 20, 42119 Wuppertal, Germany*

[6]*Turin Polytechnic University in Tashkent, Laboratory for Advanced Studies, 17 Niyazov Street, Tashkent 100095, Uzbekistan*

(Received 17 February 2021; accepted 30 March 2021; published 21 April 2021)

We consider the problem of the absence of backscattering in the transport of Manakov solitons on a line. The concept of transparent boundary conditions is used for modeling the reflectionless propagation of Manakov vector solitons in a one-dimensional domain. Artificial boundary conditions that ensure the absence of backscattering are derived and their numerical implementation is demonstrated.

DOI: 10.1103/PhysRevE.103.043305

I. INTRODUCTION

The Manakov system is an integrable system of coupled nonlinear Schrödinger equations (NLSEs) which allows different soliton solutions. The main application of the Manakov system comes from nonlinear optics, where it describes optical vector solitons propagating in Kerr media [1,2]. Manakov-type vector solitons also appear in optical fibers, in Bose-Einstein condensation, and in other areas of physics (see, e.g., Refs. [1,2] for an overview). So far, different aspects of the vector solitons described by the Manakov system have been studied [3–12]. In [13] an experimental realization of such solitons in crystals was studied. The effect of small perturbations on the collision of vector solitons and its application to ultrafast soliton switching devices was investigated in [14]. The realization of logic gates and computational operations using Manakov vector solitons was discussed in [15]. The suppression of Manakov soliton interference in optical fibers caused by the interaction of two vector solitons in the Manakov equations that govern pulse transmission in randomly birefringent fibers was studied in [16]. Reference [17] studied the rogue waves described by the Manakov system with variable coefficients and external potential.

In most cases, vector solitons are used as signal carriers in optics and optoelectronic technologies. For effective signal transmission in such devices and optimization of their functional properties, signal losses must be avoided or minimized by achieving a minimum of soliton backscattering, i.e., by propagating the solitons without reflections. The successful solution of such a problem requires the construction of mathematical models describing the reflectionless transport of solitons in a given medium. One of the effective mathematical tools for solving the problem of reflectionless soliton propagation is the imposition of so-called transparent boundary conditions (TBCs) on a wave equation describing soliton transport. For special cases of the NLSE it is possible to formulate the exact TBC in closed form (cf. [18]). For nonlinear wave equations, the concept of TBCs often relies on the so-called unified approach [19] that is based on a splitting procedure of the linear and nonlinear parts. However, in general, for NLSE-type equations, it has turned out that the so-called potential approach [20] is the most tractable one. Here we extend this promising concept to the integrable Manakov system, which is a coupled system of NLSEs with vector soliton solutions.

This paper is organized as follows. In the next section we briefly recall soliton solutions and conserving quantities for the Manakov system on a line. Section III presents the derivation of the transparent boundary conditions for the Manakov system. In Sec. IV we demonstrate our numerical implementation of such complicated boundary conditions. Section V provides a numerical experiment, which confirms obtained results. We summarize in Sec. VI.

II. SOLITON SOLUTIONS OF THE MANAKOV SYSTEM

The Manakov system can be written explicitly as

$$\begin{aligned} i\partial_t \Psi_1 + \tfrac{1}{2}\partial_x^2 \Psi_1 + (|\Psi_1|^2 + |\Psi_2|^2)\Psi_1 = 0, \\ i\partial_t \Psi_2 + \tfrac{1}{2}\partial_x^2 \Psi_2 + (|\Psi_1|^2 + |\Psi_2|^2)\Psi_2 = 0, \end{aligned} \tag{1}$$

where $(\Psi_1, \Psi_2) = (\Psi_1(x,t), \Psi_2(x,t))$, $x \in \mathbb{R}$, $t > 0$. It was introduced first by Manakov [21] to describe stationary self-focusing electromagnetic waves in homogeneous waveguide channels. The one-soliton solution of the Manakov system can be written as

$$(\Psi_1^*, \Psi_2^*) = i\Big(\frac{c}{|c|}\Big)\frac{\eta \exp|2i(\eta^2 - \xi^2)t - 2ix\xi|}{\cosh[2\eta(x + x_0 + 2\xi t)]}, \tag{2}$$

where the initial position of the soliton is given by $x_0 = \ln(2\eta/|c|)/2\eta$ and the unit vector $[c \equiv (c_{11}, c_{21})]$ determines the polarization of the soliton. The parameters ξ and η denote the speed and amplitude of the soliton, respectively.

Multisoliton solutions of the Manakov system can be obtained using Hirota's bilinearization method [22,23]. Equation (1) approves two conserving quantities, such as the norm determined as

$$N = \int_{-\infty}^{\infty} (|\Psi_1|^2 + |\Psi_2|^2) dx$$

and the energy, which is given by (cf. [24])

$$E = \int_{-\infty}^{+\infty} \left(\sum_{m=1}^{2} \frac{1}{2} \left| \frac{\partial \Psi_m}{\partial x} \right|^2 - \frac{1}{2} \sum_{m=1}^{2} |\Psi_m|^4 - |\Psi_1|^2 |\Psi_2|^2 \right) dx. \tag{3}$$

In the following we will use these quantities for confirming reflectionless transmission of Manakov solitons through a given boundary.

III. TRANSPARENT BOUNDARY CONDITIONS FOR THE MANAKOV SYSTEM

The reflection of nonlinear waves at the boundary of a given domain is a practically important problem, the solution of which requires the use of an explicit solution of a wave equation describing these waves. The mathematical description of the absence of reflection at the boundary is a rather complicated task, since unlike quantum mechanics, no S-matrix theory exists for nonlinear waves. One of the effective approaches to solve such a problem can be done in the framework of the concept of transparent boundary conditions. Such transparent boundary conditions for evolution equations can be constructed by coupling the solutions of the initial-value boundary problems in the interior and exterior domains [25–38].

To construct TBCs for a given partial differential equation (PDE), one must first split the original wave equation into coupled equations determined in the interior (Ω^{int}) and exterior (Ω^{ext}) domains. Then one applies a Laplace transform in time to the exterior problems and obtains the solution of the ordinary differential equations in the spatial variable x. Moreover, if one allows only outgoing waves by choosing the asymptotically decaying solution as $x \to \pm\infty$ and matching the Dirichlet and Neumann values on the artificial boundaries of the interior domain, one should apply (numerically) the inverse Laplace transform to complete the full derivation of the TBC [31].

Here we will apply the above concept and procedure for the derivation of TBCs for the Manakov system (1) and their numerical implementation at the artificial boundary points $x = 0$ and $x = L$. For this purpose, we use the so-called potential approach, which was previously used to derive TBCs for the nonlinear Schrödinger equation [20,39] and the sine-Gordon equation [40]. In [41–43] the TBC concept was used to develop the transparent quantum graph model, which was later implemented to describe reflectionless transport of charge carriers in branched conducting polymers [44]. Within such an approach, the Manakov system (1) is formally reduced to a system of linear PDEs

$$\begin{aligned} i\partial_t \Psi_1 + \tfrac{1}{2}\partial_x^2 \Psi_1 + V(x,t)\Psi_1 = 0, \\ i\partial_t \Psi_2 + \tfrac{1}{2}\partial_x^2 \Psi_2 + V(x,t)\Psi_2 = 0, \end{aligned} \tag{4}$$

where the potential $V(x,t)$ is given as

$$V(x,t) = |\Psi_1|^2 + |\Psi_2|^2.$$

We also introduce the new vector function as

$$\begin{aligned} v(x,t) &= e^{-i\nu(x,t)}\Psi(x,t), \\ \Psi(x,t) &= \begin{pmatrix} \Psi_1(x,t) \\ \Psi_2(x,t) \end{pmatrix}, \quad v(x,t) = \begin{pmatrix} v_1(x,t) \\ v_2(x,t) \end{pmatrix}, \end{aligned} \tag{5}$$

where

$$\begin{aligned} \nu(x,t) &= \int_0^t V(x,\tau) d\tau \\ &= \int_0^t [|\Psi_1(x,\tau)|^2 + |\Psi_2(x,\tau)|^2] d\tau. \end{aligned} \tag{6}$$

Taking here partial derivatives, we obtain

$$\begin{aligned} \partial_t \Psi &= e^{i\nu}(\partial_t + iV)v, \\ \partial_x^2 \Psi &= e^{i\nu}\left(\partial_x^2 + 2i\partial_x \nu \partial_x + i\partial_x^2 \nu - (\partial_x \nu)^2\right)v. \end{aligned}$$

Inserting these equations in (4), we get

$$L(x,t,\partial_x,\partial_t)v = i\partial_t v + \tfrac{1}{2}\partial_x^2 v + A\partial_x v + Bv = 0, \tag{7}$$

where $A = i\partial_x \nu$ and $B = \frac{1}{2}[i\partial_x^2 \nu - (\partial_x \nu)^2]$. Linearizing Eq. (7) using pseudodifferential operator calculus (see, e.g., [45,46]), we have

$$\begin{aligned} L &= \left(\frac{1}{\sqrt{2}}\partial_x + i\Lambda^-\right)\left(\frac{1}{\sqrt{2}}\partial_x + i\Lambda^+\right) \\ &= \frac{1}{2}\partial_x^2 + \frac{i}{\sqrt{2}}(\Lambda^+ + \Lambda^-)\partial_x + \frac{i}{\sqrt{2}}\mathrm{Op}(\partial_x \lambda^+) - \Lambda^-\Lambda^+, \end{aligned} \tag{8}$$

where λ^+ is the principal symbol of the operator Λ^+ and $\mathrm{Op}(p)$ denotes the associated operator of a symbol p. From Eqs. (7) and (8) we obtain the system of operators

$$\begin{aligned} \frac{i}{\sqrt{2}}(\Lambda^+ + \Lambda^-) &= A, \\ \frac{i}{\sqrt{2}}\mathrm{Op}(\partial_x \lambda^+) - \Lambda^-\Lambda^+ &= i\partial_t + B, \end{aligned} \tag{9}$$

which yields the symbolic system of equations

$$\begin{aligned} \frac{i}{\sqrt{2}}(\lambda^+ + \lambda^-) &= a, \\ \frac{i}{\sqrt{2}}\partial_x \lambda^+ - \sum_{\alpha=0}^{+\infty} \frac{(-i)^\alpha}{\alpha!}\partial_\tau^\alpha \lambda^- \partial_t^\alpha \lambda^+ &= -\tau + b, \end{aligned} \tag{10}$$

where $\mathrm{Op}(a) = A$ and $\mathrm{Op}(b) = B$ can be set as $a = A$ and $b = B$ due to the fact that these two functions correspond to zeroth-order operators. An asymptotic expansion in the inhomogeneous symbols is defined as

$$\lambda^\pm \sim \sum_{j=0}^{+\infty} \lambda^\pm_{1/2-j/2}. \tag{11}$$

Inserting the expansion (11) into Eq. (10), we can identify the terms of order $1/2$ in the first relation of the system (10):

$$\lambda_{1/2}^{-} = -\lambda_{1/2}^{+}, \quad \lambda_{1/2}^{+} = \pm\sqrt{-\tau}. \tag{12}$$

The Dirichlet-to-Neumann operator corresponds to the choice $\lambda_{1/2}^{+} = -\sqrt{-\tau}$. For the zeroth-order terms we obtain

$$\begin{aligned} \lambda_0^{-} &= -\lambda_0^{+} - i\sqrt{2}a, \\ \frac{i}{\sqrt{2}}\partial_x\lambda_{1/2}^{+} - (\lambda_0^{-}\lambda_{1/2}^{+} + \lambda_0^{+}\lambda_{1/2}^{-}) &= 0. \end{aligned} \tag{13}$$

From Eq. (13) we get

$$\begin{aligned} \lambda_0^{+} &= -i\frac{\sqrt{2}}{2}a = \frac{\sqrt{2}}{2}\partial_x\nu, \\ \lambda_0^{-} &= -\lambda_0^{+} - i\sqrt{2}a = \frac{\sqrt{2}}{2}\partial_x\nu. \end{aligned} \tag{14}$$

For the terms of order $-1/2$ we have

$$\begin{aligned} \frac{i}{\sqrt{2}}(\lambda_{-1/2}^{+} + \lambda_{-1/2}^{-}) &= 0, \\ 1\frac{i}{\sqrt{2}}\partial_x\lambda_0^{+} - (\lambda_{1/2}^{-}\lambda_{-1/2}^{+} + \lambda_0^{-}\lambda_0^{+} + \lambda_{-1/2}^{-}\lambda_{1/2}^{+}) &= b, \end{aligned} \tag{15}$$

since $\partial_t^{\alpha}\lambda_{-1/2}^{\pm} = \partial_\tau^{\alpha}\lambda_0^{\pm} = 0$, $\alpha \in N$. From (15) we get

$$\lambda_{-1/2}^{\pm} = 0. \tag{16}$$

Furthermore, one can obtain the next-order terms as

$$\lambda_{-1}^{-} = -\lambda_{-1}^{+}, \ \lambda_{-1}^{+} = i\frac{\sqrt{2}}{8\tau}\partial_x V. \tag{17}$$

Then the first-order approximation reads

$$\begin{aligned} &\frac{1}{\sqrt{2}}\partial_x\Psi_1|_{x=0} - e^{-i\pi/4}e^{i\nu}\partial_t^{1/2}(e^{-i\nu}\Psi_1)|_{x=0} = 0, \\ &\frac{1}{\sqrt{2}}\partial_x\Psi_2|_{x=0} - e^{-i\pi/4}e^{i\nu}\partial_t^{1/2}(e^{-i\nu}\Psi_2)|_{x=0} = 0, \end{aligned} \tag{18}$$

$$\begin{aligned} &\frac{1}{\sqrt{2}}\partial_x\Psi_1|_{x=L} + e^{-i\pi/4}e^{i\nu}\partial_t^{1/2}(e^{-i\nu}\Psi_1)|_{x=L} = 0, \\ &\frac{1}{\sqrt{2}}\partial_x\Psi_2|_{x=L} + e^{-i\pi/4}e^{i\nu}\partial_t^{1/2}(e^{-i\nu}\Psi_2)|_{x=L} = 0. \end{aligned} \tag{19}$$

The second-order approximation is

$$\begin{aligned} &\frac{1}{\sqrt{2}}\partial_x\Psi_1|_{x=0} - e^{-i\pi/4}e^{i\nu}\partial_t^{1/2}(e^{-i\nu}\Psi_1)|_{x=0} \\ &\quad - i\frac{\sqrt{2}}{8}\partial_x V e^{i\nu} I_t(e^{-i\nu}\Psi_1)|_{x=0} = 0, \\ &\frac{1}{\sqrt{2}}\partial_x\Psi_2|_{x=0} - e^{-i\pi/4}e^{i\nu}\partial_t^{1/2}(e^{-i\nu}\Psi_2)|_{x=0} \\ &\quad - i\frac{\sqrt{2}}{8}\partial_x V e^{i\nu} I_t(e^{-i\nu}\Psi_2)|_{x=0} = 0, \end{aligned} \tag{20}$$

$$\begin{aligned} &\frac{1}{\sqrt{2}}\partial_x\Psi_1|_{x=L} + e^{-i\pi/4}e^{i\nu}\partial_t^{1/2}(e^{-i\nu}\Psi_1)|_{x=L} \\ &\quad + i\frac{\sqrt{2}}{8}\partial_x V e^{i\nu} I_t(e^{-i\nu}\Psi_1)|_{x=L} = 0, \\ &\frac{1}{\sqrt{2}}\partial_x\Psi_2|_{x=L} + e^{-i\pi/4}e^{i\nu}\partial_t^{1/2}(e^{-i\nu}\Psi_2)|_{x=L} \\ &\quad + i\frac{\sqrt{2}}{8}\partial_x V e^{i\nu} I_t(e^{-i\nu}\Psi_2)|_{x=L} = 0, \end{aligned} \tag{21}$$

where $I_t(f) = \int_0^t f(\tau)d\tau$. Unlike the standard Dirichlet, Neumann, or Robin boundary conditions, the boundary conditions given by Eqs. (19) and (21) are quite complicated and can be implemented only numerically. Therefore, we will provide in the next section their numerical implementation for the Manakov system (1).

IV. DISCRETIZATION OF THE MANAKOV SYSTEM AND TRANSPARENT BOUNDARY CONDITIONS

For the numerical solution of the system (1) by imposing transparent boundary conditions given by Eqs. (19) and (21) one must use an effective discretization scheme for both Eq. (1) and the boundary conditions. In the case of transparent boundary conditions, the accuracy and stability of the numerical solution are very sensitive to the choice of a discretization scheme. Here we present a numerical scheme for Eq. (1) and a procedure for implementing the transparent boundary conditions.

A. Discretization of the equation

The numerical solution of coupled Schrödinger equations is a well-studied problem and different high-accuracy numerical methods have been developed in the literature so far (see, e.g., [47–51]). Here we use the explicit midpoint rule [52], the so-called leapfrog finite-difference method, which is given as

$$\begin{aligned} i\frac{\Psi_{1,j}^{n+1} - \Psi_{1,j}^{n-1}}{2\Delta t} + \frac{1}{2}D_x^2\Psi_{1,j}^{n} + V_j^{n}\Psi_{1,j}^{n} &= 0, \\ i\frac{\Psi_{2,j}^{n+1} - \Psi_{2,j}^{n-1}}{2\Delta t} + \frac{1}{2}D_x^2\Psi_{2,j}^{n} + V_j^{n}\Psi_{2,j}^{n} &= 0, \end{aligned} \tag{22}$$

with the standard second-order difference quotient

$$D_x^2\Psi_j^n = \frac{1}{\Delta x^2}\left(\Psi_{j+1}^n - 2\Psi_j^n + \Psi_{j-1}^n\right)$$

and the discrete potential term

$$V_j^n = \left|\Psi_{1,j}^n\right|^2 + \left|\Psi_{2,j}^n\right|^2,$$

where Δt and Δx are the time and space discretization steps, respectively. We note that there are other implicit or semi-implicit methods with higher accuracy [50–55]; however, the complexity of the TBC forces us to choose between accuracy and computational cost. This method was chosen because of its simple implementation and low cost per step. This leads to the explicit finite-difference scheme

$$\mathbf{U}_j^{n+1} = \mathbf{U}_j^{n-1} + i\Delta t D_x^2\mathbf{U}_j^n + 2i\Delta t V_j^n\mathbf{U}_j^n, \tag{23}$$

where

$$\mathbf{U}_j^n = \begin{pmatrix} \Psi_{1,j}^n \\ \Psi_{2,j}^n \end{pmatrix}.$$

Furthermore, we have to implement the transparent boundary conditions given by Eqs. (18) and (19) or Eqs. (20) and (21) in the above numerical methods.

B. Implementation of the TBC

The discretization of the TBC given by Eqs. (18) and (19), its subsequent implementation in the numerical scheme for Eq. (1), and ensuring the stability of the whole numerical scheme is a rather complicated task. The presence of the fractional derivative also makes the discretization scheme very complicated and unstable. Therefore, one must find a suitable numerical scheme that is stable when combined with the transparent boundary conditions. To achieve this, one must perform a stability analysis for a chosen discretization scheme to study its stability. Here we give an effective discretization scheme for the TBC that can be implemented with high accuracy and stability when combined with the discretization scheme for Eq. (1). We state the scheme only for $x = L$ by saying that for the left boundary (at $x = 0$) the implementation can be done in the same way.

The approximation of the fractional differential operator is given by the numerical quadrature formula [20]

$$\partial_t^{1/2} f(t_n) \approx \frac{2}{\sqrt{2\Delta t}} \sum_{k=0}^{n} \beta_k f^{n-k},$$

where $\{f_n\}_{n\in\mathbb{N}}$ is a sequence of complex values approximating $\{f(t_n)\}_{n\in\mathbb{N}}$ and $(\beta_k)_{k\in\mathbb{N}}$ denotes the sequences defined by

$$(\beta_0, \beta_1, \beta_2, \beta_3, \beta_4, \beta_5, \ldots) = \left(1, -1, \frac{1}{2}, -\frac{1}{2}, \frac{1\times 3}{2\times 4}, -\frac{1\times 3}{2\times 4}, \ldots\right).$$

The function $v(x,t)$ given by (6) can be discretized using the trapezoidal rule as

$$v_j^n = \Delta t\left[\sum_{k=1}^{n-1} V_j^k + \frac{1}{2}V_j^n\right] \quad \text{for } n \geqslant 2,$$

with $v_j^0 = 0$ and $v_j^1 = \frac{\Delta t}{2} V_j^1$. Let us note that the term $\frac{1}{2}V_0^n$ was dropped because the initial data are assumed to be compactly supported and hence V_0^n is zero. Then we discretize the function $e^{iv(x,t)}$ from (5) as

$$\begin{aligned} E_j^n &= \exp\left(iv_j^n\right) \\ &= \exp\left(i\Delta t \sum_{k=1}^{n-1} V_j^k\right) \exp\left(i\Delta t \frac{1}{2} V_j^n\right) \\ &= \widetilde{E_j^{n-1}} \exp\left(i\Delta t \frac{1}{2} V_j^n\right), \end{aligned}$$

where $\widetilde{E_j^{n-1}} = \exp(i\Delta t \sum_{k=1}^{n-1} V_j^k)$. Thus, the TBC operator of the first-order approximation (19) at the right boundary $j = J$ can be approximated by the discrete convolutions

$$\begin{aligned} \left(\Lambda_1^n\right)_I &= e^{-i\pi/4}\sqrt{\frac{2}{\Delta t}} E_J^n \sum_{k=0}^{n} \beta_k \overline{E_J^{n-k}} \Psi_{1,J}^{n-k}, \\ \left(\Lambda_2^n\right)_I &= e^{-i\pi/4}\sqrt{\frac{2}{\Delta t}} E_J^n \sum_{k=0}^{n} \beta_k \overline{E_J^{n-k}} \Psi_{2,J}^{n-k}, \end{aligned}$$

where $\overline{E_J^n}$ denotes the complex conjugate of E_J^n. Then the values of the wave function at the right boundary can be obtained by solving the system of nonlinear equations with respect to $(\Psi_{1,J}^n, \Psi_{2,J}^n)^\top$, given as

$$\begin{aligned} &\frac{\Psi_{1,J}^n - \Psi_{1,J-1}^n}{\Delta x} + e^{-i\pi/4}\frac{2}{\sqrt{\Delta t}}\Big[\Psi_{1,J}^n + \widetilde{E_J^{n-1}} \\ &\quad \times \exp\left(i\frac{\Delta t}{2}\left(\left|\Psi_{1,J}^n\right|^2 + \left|\Psi_{2,J}^n\right|^2\right)\right)\sum_{k=1}^{n} \beta_k \overline{E_J^{n-k}} \Psi_{1,J}^{n-k}\Big] = 0, \end{aligned}$$

$$\begin{aligned} &\frac{\Psi_{2,J}^n - \Psi_{2,J-1}^n}{\Delta x} + e^{-i\pi/4}\frac{2}{\sqrt{\Delta t}}\Big[\Psi_{2,J}^n + \widetilde{E_J^{n-1}} \\ &\quad \times \exp\left(i\frac{\Delta t}{2}\left(\left|\Psi_{1,J}^n\right|^2 + \left|\Psi_{2,J}^n\right|^2\right)\right)\sum_{k=1}^{n} \beta_k \overline{E_J^{n-k}} \Psi_{2,J}^{n-k}\Big] = 0. \end{aligned}$$

Using the same approach, we can proceed with the discretization of the second-order approximation. We recall that $V(x,t) = \overline{\Psi}_1\Psi_1 + \overline{\Psi}_2\Psi_2$ and approximate $\partial_x V(x,t)$ at the right boundary $x = L$ (i.e., $j = J$) with

$$\begin{aligned} dV_J^n = \frac{1}{\Delta x}\big(&2|\Psi_{1,J}^n|^2 - \overline{\Psi_{1,J-1}^n}\Psi_{1,J}^n - \Psi_{1,J-1}^n\overline{\Psi_{1,J}^n} \\ &+ 2|\Psi_{2,J}^n|^2 - \overline{\Psi_{2,J-1}^n}\Psi_{2,J}^n - \Psi_{2,J-1}^n\overline{\Psi_{2,J}^n}\big), \end{aligned}$$

where $\overline{\Psi}$ is the complex conjugate of Ψ. Then, again using the trapezoidal method, we approximate the integral term $I_t(\cdot)$ in (21) with

$$I_{m,t}^n = \Delta t\left(\sum_{k=1}^{n-1} \overline{E_J^k}\Psi_{m,J}^k + \frac{1}{2}\overline{E_J^n}\Psi_{m,J}^n\right), \quad m = 1, 2.$$

Thus, the TBC operator of the second-order approximation (21) can be approximated as

$$\begin{aligned} \left(\Lambda_1^n\right)_{II} &= \left(\Lambda_1^n\right)_I + i\frac{\sqrt{2}}{8} dV_J^n E_J^n I_{1,t}^n, \\ \left(\Lambda_2^n\right)_{II} &= \left(\Lambda_2^n\right)_I + i\frac{\sqrt{2}}{8} dV_J^n E_J^n I_{2,t}^n. \end{aligned}$$

Again, the values of the wave function at the right boundary can be obtained by solving the system of nonlinear equations with respect to $(\Psi_{1,J}^n, \Psi_{2,J}^n)^\top$, given as

$$\begin{aligned} &\frac{\Psi_{1,J}^n - \Psi_{1,J-1}^n}{\Delta x} + e^{-i\pi/4}\frac{2}{\sqrt{\Delta t}}\Big[\Psi_{1,J}^n + \widetilde{E_J^{n-1}} \\ &\quad \times \exp\left(i\frac{\Delta t}{2}\left(\left|\Psi_{1,J}^n\right|^2 + \left|\Psi_{2,J}^n\right|^2\right)\right)\sum_{k=1}^{n} \beta_k \overline{E_J^{n-k}} \Psi_{1,J}^{n-k}\Big] \\ &\quad + i\frac{\Delta t}{4\Delta x}\Big(2\left|\Psi_{1,J}^n\right|^2 - \overline{\Psi_{1,J-1}^n}\Psi_{1,J}^n - \Psi_{1,J-1}^n\overline{\Psi_{1,J}^n} \\ &\quad + 2\left|\Psi_{2,J}^n\right|^2 - \overline{\Psi_{2,J-1}^n}\Psi_{2,J}^n - \Psi_{2,J-1}^n\overline{\Psi_{2,J}^n}\Big) \\ &\quad \times \widetilde{E_J^{n-1}} \exp\left(i\frac{\Delta t}{2}\left(\left|\Psi_{1,J}^n\right|^2 + \left|\Psi_{2,J}^n\right|^2\right)\right) \\ &\quad \times \left(\sum_{k=1}^{n-1} \overline{E_J^k}\Psi_{1,J}^k + \frac{1}{2}\overline{E_J^n}\Psi_{1,J}^n\right) = 0, \end{aligned}$$

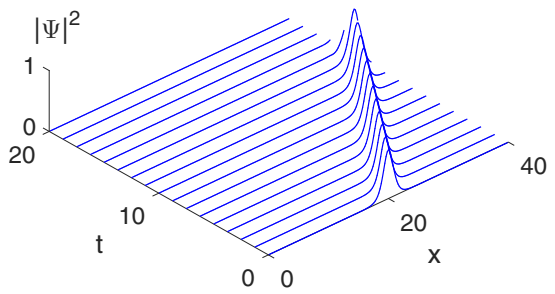

FIG. 1. Evolution of a right-traveling single soliton simulated with the finite-difference scheme (23). The first-order approximation of the TBC is imposed at the right boundary ($x = 40$).

$$\frac{\Psi^n_{2,J} - \Psi^n_{2,J-1}}{\Delta x} + e^{-i\pi/4}\frac{2}{\sqrt{\Delta t}}\Big[\Psi^n_{2,J} + \widetilde{E^{n-1}_J} \times \exp\Big(i\frac{\Delta t}{2}(|\Psi^n_{1,J}|^2 + |\Psi^n_{2,J}|^2)\Big)\sum_{k=1}^{n}\beta_k\overline{E^{n-k}_J}\Psi^{n-k}_{2,J}\Big] + i\frac{\Delta t}{4\Delta x}\Big(2|\Psi^n_{1,J}|^2 - \overline{\Psi^n_{1,J-1}}\Psi^n_{1,J} - \Psi^n_{1,J-1}\overline{\Psi^n_{1,J}} + 2|\Psi^n_{2,J}|^2 - \overline{\Psi^n_{2,J-1}}\Psi^n_{2,J} - \Psi^n_{2,J-1}\overline{\Psi^n_{2,J}}\Big) \times \widetilde{E^{n-1}_J}\exp\Big(i\frac{\Delta t}{2}(|\Psi^n_{1,J}|^2 + |\Psi^n_{2,J}|^2)\Big) \times \left(\sum_{k=1}^{n-1}\overline{E^k_J}\Psi^k_{2,J} + \frac{1}{2}\overline{E^n_J}\Psi^n_{2,J}\right) = 0.$$

V. NUMERICAL EXPERIMENT

We solve the system of coupled nonlinear Schrödinger equations, given by Eq. (1) on the finite interval $[0, L]$, and impose the TBC at the right boundary (at $x = L$). As the initial condition we choose a single soliton from the exact solution given by

$$\Psi_1(x, 0) = \sqrt{\alpha}\,\mathrm{sech}[\sqrt{2\alpha}(x - x_0)]\exp[i\sqrt{2}p(x - x_0)],$$
$$\Psi_2(x, 0) = \sqrt{\alpha}\,\mathrm{sech}[\sqrt{2\alpha}(x - x_0)]\exp[i\sqrt{2}p(x - x_0)].$$

In our experiments we selected the following system parameters: $L = 40$; the parameters of the initial condition $\alpha = 1$, $p = 1$, and $x_0 = 20$; and the discretization parameters $\Delta x = 0.05$ and $\Delta t = 0.001\,25$. The evolution of the right-traveling single soliton is shown in Fig. 1.

To check the the absence of backscattering, we numerically calculate and plot the time dependence of the energy given by Eq. (3). The fact that the energy becomes zero while time elapses can be considered as a marker of the TBC. Assuming that the wave function determined by the initial conditions is negligibly small outside the computational domain $[0, L]$, Eq. (3) can be rewritten as

$$E = \frac{1}{2}\int_0^L \left(\sum_{m=1}^{2}\left|\frac{\partial\Psi_m}{\partial x}\right|^2 - (|\Psi_1|^2 + |\Psi_2|^2)^2\right)dx. \qquad (24)$$

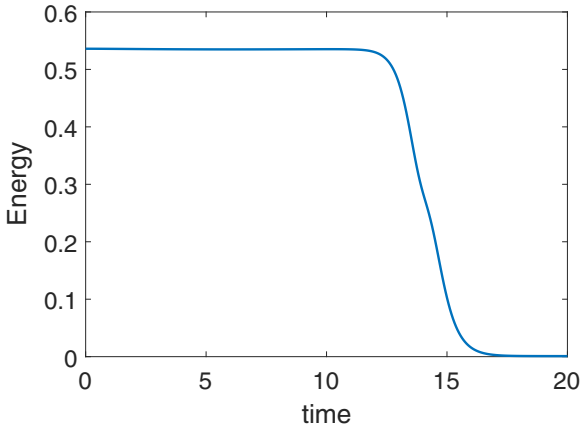

FIG. 2. Time evolution of the soliton energy in the interior (computational) domain $[0, L]$.

In our calculations we use the discrete analog of the energy $[E(t_n) = E_n]$ given by Eq. (24):

$$E_n = \frac{1}{4\Delta x}\sum_{j=1}^{J-1}\Big[\big|\Psi^n_{1,j+1} - \Psi^n_{1,j-1}\big|^2 + \big|\Psi^n_{2,j+1} - \Psi^n_{2,j-1}\big|^2 - 2\Delta x^2\big(\big|\Psi^n_{1,j}\big|^2 + \big|\Psi^n_{2,j}\big|^2\big)^2\Big].$$

The time evolution of the soliton energy within the limits of the calculation interval is shown in Fig. 2. It is clear that the energy disappears when the soliton crosses the boundary, i.e., the absence of backscattering.

At the end, to show that the numerical solution is reliable, we calculate the absolute error $\mathcal{E}$, i.e., the difference of the numerical solution to the exact analytical solution, measured with the L^2-norm (discretized by the trapezoidal rule)

$$\|\mathcal{E}(t_n)\|_2^2 = \Delta x\sum_{j=1}^{J-1}\big(\big|\Delta\Psi^n_{1,j}\big|^2 + \big|\Delta\Psi^n_{2,j}\big|^2\big) + \frac{\Delta x}{2}\big(\big|\Delta\Psi^n_{1,0}\big|^2 + \big|\Delta\Psi^n_{2,0}\big|^2 + \big|\Delta\Psi^n_{1,J}\big|^2 + \big|\Delta\Psi^n_{2,J}\big|^2\big),$$

where $\Delta\Psi^n_{k,j} = \Psi^n_{k,j} - \Psi^{\mathrm{exact}}_k(x_j, t_n)$. The plot of this error over time is presented in Fig. 3 (red line). Since this error consists of two different errors caused by the approximation

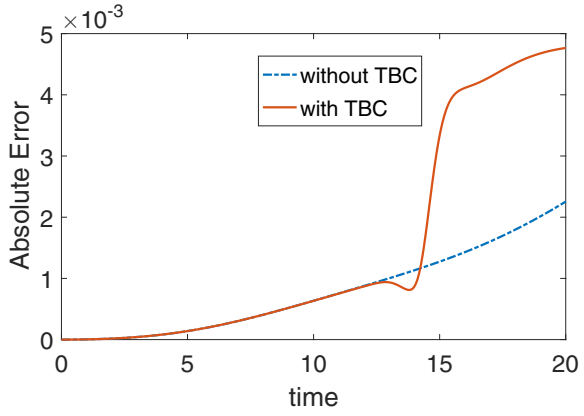

FIG. 3. Plot of the absolute error in the L^2-norm.

and discretization of the TBC and by the discretization error of the finite-difference scheme, for comparison we plot a second error labeled "without TBC" where we compute the solution for an extended interval $[0, 2L]$ (such that the right boundary is not reached within the considered time frame). In other words, the blue curve in Fig. 3 shows the unavoidable error due to the interior scheme and we observe that the additional error due to the approximated TBC is within the same magnitude of 10^{-3}.

VI. CONCLUSION

In this work, the reflectionless transmission of Manakov solitons described by the Manakov system on a line subject to so-called transparent boundary conditions has been studied. These transparent boundary conditions were derived analytically and an effective discretization for the TBCs and its implementation in the numerical method for the Manakov system were presented. The absence of backscattering for Manakov solitons, when TBCs are imposed, was demonstrated by a direct numerical experiment. The results of the work can be used for modeling the tunable transport of Manakov solitons in optical media and for optimization problems of optical devices, where such solitons appear as signal carriers. We note that imposing transparent boundary conditions on real physical systems is a rather complicated task caused by the very complicated form of the TBCs. However, in some cases it may be possible to find some physically realistic boundary conditions equivalent to the transparent ones. It is clear that such an equivalence is not general and it can be assumed only under certain constraints. Earlier, such equivalent and physically acceptable boundary conditions were found, for example, for the nonlinear (one-component) Schrödinger equation on metric graphs in Ref. [39] and for some linear wave equations in [43,44]. Finally, we found that the above model can be extended to model reflectionless propagation of Manakov vector solitons in higher-dimensional and branched domains, which is a task left for future work.

[1] Y. S. Kivshar and G. P. Agrawal, *Optical Solitons: From Fibers to Photonic Crystals* (Academic, San Diego, 2003).
[2] G. P. Agrawal, *Applications of Nonlinear Fiber Optics* (Academic, San Diego, 2001).
[3] R. Radhakrishnan, M. Lakshmanan, and J. Hietarinta, Phys. Rev. E **56**, 2213 (1997).
[4] T. Kanna and M. Lakshmanan, Phys. Rev. Lett. **86**, 5043 (2001).
[5] M. J. Ablowitz, B. Prinari, and A. D. Trubatch, Inv. Probl. **20**, 1217 (2004).
[6] R. Radhakrishnan and M. Lakshmanan, J. Phys. A: Math. Gen. **28**, 2683 (1995).
[7] A. P. Sheppard and Y. S. Kivshar, Phys. Rev. E **55**, 4773 (1997).
[8] M. Vijayajayanthi, T. Kanna, and M. Lakshmanan, Phys. Rev. A **77**, 013820 (2008).
[9] B. F. Feng, J. Phys. A: Math. Theor. **47**, 355203 (2014).
[10] Y. Ohta, D. S. Wang, and J. Yang, Stud. Appl. Math. **127**, 345 (2011).
[11] P. G. Kevrekidis and D. J. Frantzeskakis, Rev. Phys. **1**, 140 (2016).
[12] D. J. Frantzeskakis, J. Phys. A: Math. Theor. **43**, 213001 (2010).
[13] J. U. Kang, G. I. Stegeman, J. S. Aitchison, and N. Akhmediev, Phys. Rev. Lett. **76**, 3699 (1996).
[14] J. Yang, Phys. Rev. E **59**, 2393 (1999).
[15] K. Steiglitz, Phys. Rev. E **63**, 016608 (2000).
[16] J. Yang, Phys. Rev. E **65**, 036606 (2002).
[17] W.-P. Zhong, M. Belić, and B. A. Malomed, Phys. Rev. E **92**, 053201 (2015).
[18] C. Zheng, J. Comput. Phys. **215**, 552 (2006).
[19] H. Li, X. Wu, and J. Zhang, Phys. Rev. E **84**, 036707 (2011).
[20] X. Antoine, C. Besse, and S. Descombes, SIAM J. Numer. Anal. **43**, 2272 (2006).
[21] S. V. Manakov, Sov. Phys. JETP **38**, 248 (1974).
[22] S. Gancsan and M. Lakshmanan, J. Phys. A: Math. Gen. **20**, L1143 (1987).
[23] M. Lakshmanan, Int. J. Bifurcat. Chaos **3**, 3 (1993).
[24] M. S. Ismail, Math. Comput. Simul. **78**, 532 (2008).
[25] A. Arnold and M. Ehrhardt, J. Comput. Phys. **145**, 611 (1998).
[26] M. Ehrhardt, VLSI Design **9**, 325 (1999).
[27] M. Ehrhardt and A. Arnold, Riv. Math. Univ. Parma **6**, 57 (2001).
[28] M. Ehrhardt, Acta Acust. United Ac. **88**, 711 (2002).
[29] A. Arnold, M. Ehrhardt, and I. Sofronov, Commun. Math. Sci. **1**, 501 (2003).
[30] S. Jiang and L. Greengard, Comput. Math. Appl. **47**, 955 (2004).
[31] X. Antoine, A. Arnold, C. Besse, M. Ehrhardt, and A. Schädle, Commun. Comput. Phys. **4**, 729 (2008).
[32] M. Ehrhardt, Appl. Numer. Math. **58**, 660 (2008).
[33] A. Zisowsky and M. Ehrhardt, Math. Comput. Model. **47**, 1264 (2008).
[34] L. Šumichrast and M. Ehrhardt, J. Electr. Eng. **60**, 301 (2009).
[35] X. Antoine, C. Besse, and P. Klein, J. Comput. Phys. **228**, 312 (2009).
[36] M. Ehrhardt, Numer. Math. Theor. Meth. Appl. **3**, 295 (2010).
[37] P. Klein, X. Antoine, C. Besse, and M. Ehrhardt, Commun. Comput. Phys. **10**, 1280 (2011).
[38] A. Arnold, M. Ehrhardt, M. Schulte, and I. Sofronov, Commun. Math. Sci. **10**, 889 (2012).
[39] J. R. Yusupov, K. K. Sabirov, M. Ehrhardt, and D. U. Matrasulov, Phys. Rev. E **100**, 032204 (2019).
[40] K. K. Sabirov, J. R. Yusupov, M. Ehrhardt, and D. U. Matrasulov, arXiv:2011.13299.
[41] J. R. Yusupov, K. K. Sabirov, M. Ehrhardt, and D. U. Matrasulov, Phys. Lett. A **383**, 2382 (2019).
[42] M. M. Aripov, K. K. Sabirov, and J. R. Yusupov, Nanosyst.: Phys. Chem. Math. **10**, 501 (2019).
[43] J. R. Yusupov, K. K. Sabirov, Q. U. Asadov, M. Ehrhardt, and D. U. Matrasulov, Phys. Rev. E **101**, 062208 (2020).
[44] J. R. Yusupov, K. S. Matyokubov, K. K. Sabirov, and D. U. Matrasulov, Chem. Phys. **537**, 110861 (2020).
[45] M. Taylor, *Pseudo Differential Operators*, Lecture Notes in Mathematics Vol. 416 (Springer, Berlin, 1974).

[46] L. Nirenberg, Lectures on Linear Partial Differential Equations, CBMS Regional Conference Series in Mathematics (AMS, Providence, 1972), Vol. 17.
[47] M. S. Ismail and T. R. Taha, Math. Comput. Simul. **56**, 547 (2001).
[48] M. S. Ismail and S. Z. Alamri, Int. J. Comput. Math. **81**, 333 (2004).
[49] M. S. Ismail and T. R. Taha, Math. Comput. Simul. **74**, 302 (2007).
[50] M. S. Ismail, Math. Comput. Simul. **196**, 273 (2008).
[51] Q.-B. Xu and Q.-S. Chang, Acta Math. Appl. Sin. Engl. Ser. **26**, 205 (2010).
[52] J. de Frutos and J. M. Sanz-Serna, J. Comput. Phys. **103**, 160 (1992).
[53] S. Zhou and X. Cheng, Math. Comput. Simul. **80**, 2362 (2010).
[54] J. Chen and L.-M. Zhang, Acta Math. Appl. Sin. Engl. Ser. **33**, 435 (2017).
[55] Y. Hu, H. Li, and Z. Jiang, Appl. Numer. Math. **153**, 319 (2020).